



**COBEM**  
2021 Florianópolis - Brasil



26<sup>th</sup> ABCM International Congress of Mechanical Engineering  
November 22-26, 2021. Florianópolis, SC, Brazil

**COB-2021-1229**

## **THERMAL PERFORMANCE OF A FLAT PLATE PULSATING HEAT PIPE WITH ULTRA-SHARP LATERAL GROOVES**

**Larissa Krambeck**

**Kelvin Guessi Domiciano**

Department of Mechanical Engineering, Federal University of Santa Catarina, Florianópolis/SC, 88040-900, Brazil  
larissa.krambeck@labtucal.ufsc.br; kelvin.guessi@labtucal.ufsc.br

**Luis Alonso Betancur Arboleda**

Technological Units of Santander, Bucaramanga, Santander, Colombia  
labetancur@correo.uts.edu.co

**Marcia Barbosa Henriques Mantelli**

Department of Mechanical Engineering, Federal University of Santa Catarina, Florianópolis/SC, 88040-900, Brazil  
marcia@labtucal.ufsc.br

**Abstract.** *The thermal performance study of a new geometry ultra-sharp lateral grooved flat plate pulsating heat pipe is performed in high heat load operating conditions. This novel geometry consists of a round cross-section with ultra-sharp lateral grooves, located at the evaporator. The thermal performance is compared to ordinary flat PHP, with round cross-section channels. Diffusion bonding technology is used to manufacture the pulsating heat pipes, made of copper. The working fluid used is distilled water with a filling ratio of 60%. The pulsating heat pipes are tested at three positions: gravity-assisted, horizontal, and against-gravity, under heat loads varying from 600 to 2000 W, a value higher than the PHP's working conditions described in the literature. For large heat loads, both PHPs (round and round with ultra-sharp grooves) work successfully, able to transfer up to 2000 W. The gravity influence is negligible for power inputs beyond 1200 W for any orientation. The main difference in the thermal behavior of the grooved, when compared to the round PHPs, is related to the maximum evaporator temperature, which is reduced by almost 5°C. Also, the experimental results show that the lateral grooves improve the thermal performance of the pulsating heat pipe, reducing the thermal resistance.*

**Keywords:** *pulsating heat pipes, lateral grooves, thermal performance, experimental.*

### **1. INTRODUCTION**

The development of electronic gadgets is in fast progress, requiring more efficient thermal control technologies, which must be able to remove high heat fluxes, keeping the fabrication costs low. Pulsating heat pipes (PHP) are passive cooling devices that may fill this gap (Laun *et al.*, 2015). The PHP uses the oscillatory movement of a confined phase change working fluid to transfer heat from an evaporator to a condenser. When heat is provided at the evaporator section, bubbles start to grow in non-equilibrium conditions, moving liquid slugs from the evaporator to the condenser regions. The collapsing of the bubbles at the condenser cooperates in the liquid dislocation (Karimi and Culham, 2004). A flat plate PHP is manufactured by diffusion welding of plates in which the match of machined faces forms channels, as shown in Figure 1.

The development of flat plate PHPs has received greater attention in the recent literature. They present some promising characteristics such as: higher density of channels per unit volume (Yoon and Kim, 2014), the possibility of functionalizing the internal channel surfaces, ability to dissipate high heat fluxes and their easy coupling to the electronic equipment for cooling (Ma, 2015).

Thin liquid films over surfaces, which are formed due to surface tension action, maintain the evaporator wet, enabling the nucleation of vapor bubbles. Amendments in the channel geometry can improve the liquid pumping capacity of the PHP and, consequently, increase the PHP thermal performance, making it less dependent on gravity. Such devices are great candidates for microgravity applications.

Khandekar *et al.* (2003) and Facin *et al.* (2018) compared the performance of PHPs with rectangular and circular channels. They concluded that the capillarity of the channel edges of the rectangular geometry helps the liquid to be spread along the evaporator, improving its thermal performance.

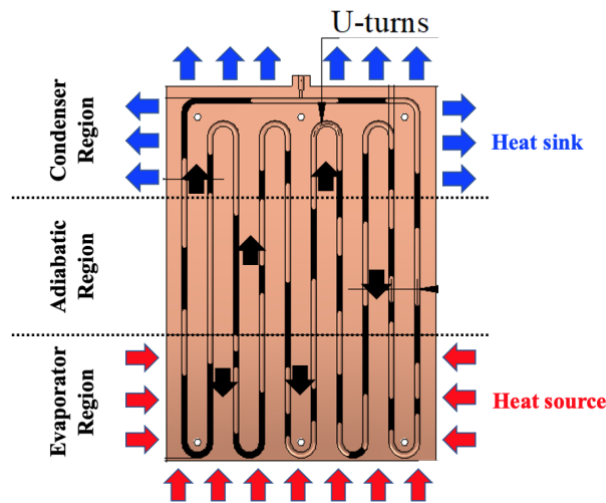


Figure 1. Schematic design of the operating principle of a flat plate PHP.

Cai *et al.* (2006) fabricated a planar PHP by compressing the top half of a copper tube. Its deformed cross-section produced a flat upper surface with two laterals microgrooves. The testing results showed that the new channel profile could improve the liquid supply at the evaporator and reduce its temperature oscillations. Qu *et al.* (2017) manufactured tubular PHPs with internal helical microgrooves. The maximum input heat flux that they tested was  $3.8 \text{ W/cm}^2$ . They observed reduced thermal resistance, showing that the device could transfer more heat. Reaching the same conclusions, Kim and Kim (2018) lowered the thermal resistance of a PHP by up to 57%, by adding four reentrant cavities with different sizes in the channel of a micro PHP. The maximum heat load was 16 W. The authors concluded that the number of nucleation sites in these cavities was large.

Several researchers focused on lower heat load PHP applications (Khandekar *et al.*, 2003; Kim and Kim, 2018; Qu *et al.*, 2017). Recently, Czajkowski *et al.* (2020) provided a new study on tubular PHP by applying heat transfer rates larger than commonly used, from 500 W ( $1.4 \text{ W/cm}^2$ ) up to 2000 W ( $5.6 \text{ W/cm}^2$ ). However, there is a lack of information about flat plate PHP operating at high heating powers. In the present work, a thermal performance study of new geometry, ultra-sharp lateral grooved flat plate PHP, is performed for high heat load applications. The novel cross-section geometry consists of a round channel with lateral ultra-sharp corners at the evaporator section. The effect of gravity is studied by performing the tests in three positions: gravity-assisted, horizontal, and against-gravity, under heat loads varying from 600 up to 2000 W (heat flux from 2.7 up to  $8.9 \text{ W/cm}^2$ ). The results are compared with those of the round channel PHP, tested under the same experimental conditions. Two major contributions are proposed in this work: a new easy to construct channel geometry and a PHP able to operate at high heat loads.

## 2. METHODOLOGY

### 2.1 The manufacturing of the pulsating heat pipes

Four flat copper plates of  $208 \times 150 \times 2.2 \text{ mm}$  were used to fabricate two PHPs. In each one, semi-circular profile channels were machined with 13 U-turns (formed by 26 interconnected parallel channels). The machined faces of the plates were joined by the diffusion bonding, forming round cross-section channels of 2.5 mm in diameter. The PHPs present an evaporator of 80 mm, an adiabatic region of 48 mm, and a condenser of 80 mm.

In the first “ordinary” PHP, two flat plates, in which grooves of semicircular cross-section shapes were drilled, were just superposed, forming the round cross-section channels. In the second one, small chamfers of  $20^\circ$  angles are drilled at the corners of the semi-circular channel. When both sides are superposed, ultra-sharp lateral grooves in the interface are formed, showing a  $40^\circ$  angle and 0.37 mm opening mouth. The grooves intend to create edges that can work as porous media and keeps the entire evaporator wet. More details about the machining, diffusion bonding process and the resulting geometry analysis are presented in Betancur *et al.* (2020). The resulting grooved PHP and the final channel’s geometries at evaporator and condenser are shown in Figure 2.

According to Hosoda *et al.* (1999), a PHP with a circular cross-section and water as working fluid performed best at a charge ratio of 60%. Therefore, in the present work, distilled degassed water, in a total volume of 18.0 ml, was used as the working fluid, corresponding to a filling ratio (FR) of 60%. The FR is defined as the ratio between the volume of liquid and the total internal volume of the PHP channels.

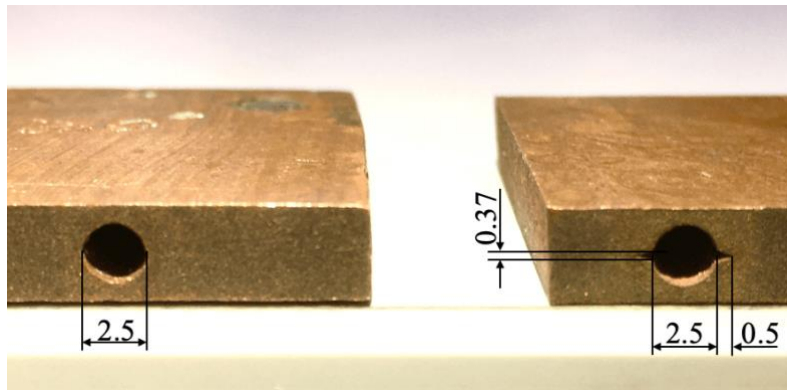


Figure 2. Channel's profiles after the diffusion bonding, round on the right side and grooved on the left side.

## 2.2 Experimental apparatus

The experimental apparatus used for the thermal tests, shown in Figure 3, is composed of a programmable power source (*TDK-Lambda*<sup>TM</sup> GEN300-17), data acquisition (*DAQ-NI*<sup>TM</sup> SCXI-1000), a *Dell*<sup>TM</sup> laptop, a thermal bath (*Lauda Proline*<sup>TM</sup> RP1845) and T-type thermocouples (*Omega Engineering*<sup>TM</sup>).

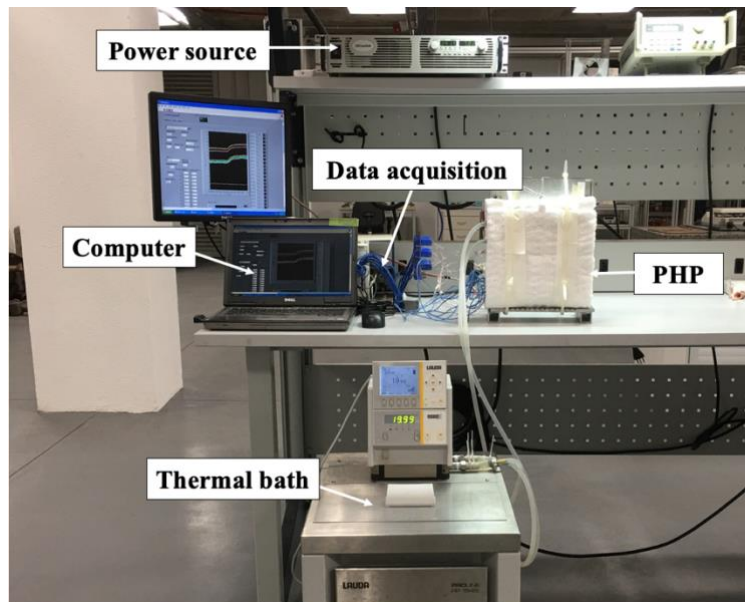


Figure 3. Experimental apparatus.

The evaporator receives power from a programmable power source through eight cartridge electrical resistances (10 mm in diameter, 100 mm in length, and 315 W) embedded on copper blocks of 140 x 20 mm<sup>2</sup>, distributed in both sides of the PHP. The condenser rejects heat through an aluminum block (140 x 80 mm<sup>2</sup>) with two parallel channels for cooling water flow. The thermal bath controls the inlet temperature. The interfacial contact area of the evaporator and condenser are 22,400 mm<sup>2</sup> and 11,200 mm<sup>2</sup>, respectively. An adiabatic section is provided between the evaporator and the condenser. Thermal grease (*Omegatherm*<sup>TM</sup> 201) reduces the contact resistance in the evaporator and the condenser. The PHP is insulated from the external ambient by an *Isoglas*<sup>TM</sup> blanket (thickness of 30 mm). Figure 4 presents the test section without the insulation for a detailed view.

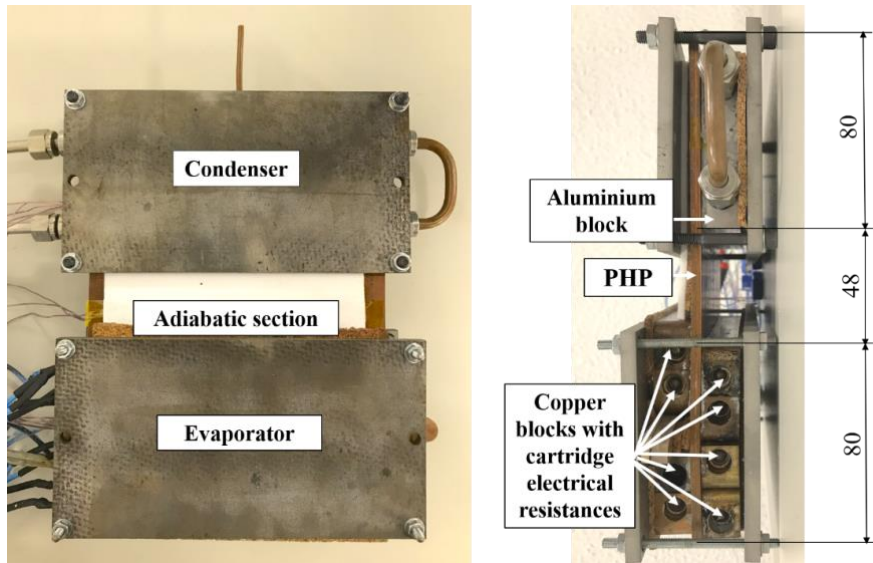


Figure 4. Experimental setup.

For the thermal evaluation of the PHPs, fourteen T-type thermocouples connected to the data acquisition system are used. The temperature sensors are fixed on the outer surface by a thermosensitive adhesive strip *Kapton*<sup>TM</sup>. The thermocouple positions in the evaporator ( $T_{\text{evap},1}$ ,  $T_{\text{evap},2}$ ,  $T_{\text{evap},3}$ ,  $T_{\text{evap},4}$ ,  $T_{\text{evap},5}$ ), the adiabatic section ( $T_{\text{adiab},1}$ ,  $T_{\text{adiab},2}$ ,  $T_{\text{adiab},3}$ ), and the condenser ( $T_{\text{cond},1}$ ,  $T_{\text{cond},2}$ ,  $T_{\text{cond},3}$ ,  $T_{\text{cond},4}$ ,  $T_{\text{cond},5}$ ) are shown in Figure 5. The last thermocouple measured the ambient temperature ( $T_{\text{amb}}$ ).

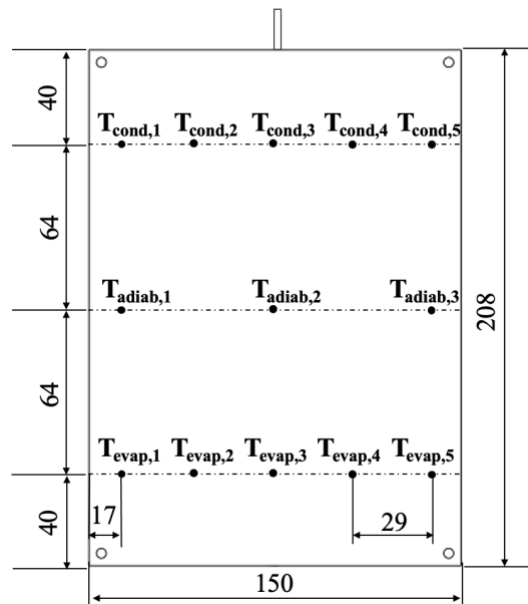


Figure 5. Thermocouple distribution.

The test procedure started setting the condenser parameters: water temperature at 20 °C and a flow rate of 20 l/min. Tests were performed increasing the heat load in steps of 200 W, ranging from 600 up to 2000 W (from 2.7 up to 8.9 W/cm<sup>2</sup>), in three positions: gravity-assisted (evaporator above condenser), horizontal, and against-gravity orientation (condenser above evaporator). The system was left for 900s at each heat input level to guarantee steady-state operation conditions. Experimental data were acquired and recorded by the *Labview*<sup>TM</sup> software at a rate of 1 sample/second.

### 2.3 Data reduction

The following parameters are evaluated for the proposed pulsating heat pipes: temperature distribution, the average temperatures and their amplitude of temperature at each section and the overall thermal resistance. The temperature

distributions were analyzed by observing the time responses of the thermocouple readings for each applied heat load. By mean temperature,  $\bar{T}$ , it is understood the average temperature of the thermocouples of each region. Amplitude is taken as the maximum minus the minimum temperature in the evaporator and the condenser:

$$\Delta T_{evap} = T_{evap, max} - T_{evap, min} \quad (1)$$

$$\Delta T_{cond} = T_{cond, max} - T_{cond, min} \quad (2)$$

The overall thermal resistance,  $R_t$ , which represents the difficulty of a heat pipe to transport the heat power, is estimated as the ratio of the average temperature difference between the evaporator and condenser and the dissipated power:

$$R_t = \frac{\bar{T}_{evap} - \bar{T}_{cond}}{q} \quad (3)$$

where  $\bar{T}_{evap}$  is the average temperature of the thermocouples located in the evaporator,  $\bar{T}_{cond}$  is the average temperature of the thermocouples at the condenser, and  $q$  stands for the heat transfer rate given by the power supply.

Thermal losses from the PHP to the environment were determined and considered negligible, as their maximum value was less than 2% of the total heat transported  $q$ .

The experimental uncertainties were calculated by the error propagation technique, according to the procedures described by Holman (2011). They were associated with measurement uncertainties of the T-type thermocouples, the data logger and the power supply. The average temperature uncertainty of each section is estimated at around  $\pm 1.46$  °C. The voltage and current measurement uncertainties, provided by the manufacturer of the power supply equipment, are 30 mV and 8.5 mA, respectively. Therefore, the thermal resistance uncertainty is lower than 7% for all the input power levels. The uncertainty ranges are shown by vertical bars in the overall thermal resistance plots.

### 3. RESULTS AND DISCUSSION

In this section, the experimental thermal performance of the ordinary round PHP is compared with the grooved new channel geometry one.

#### 3.1 Temperature distribution

Figure 6 presents the temperature distributions as a function of time for the round and the grooved PHPs, for all the orientations tested. Results showed that the two tested PHPs worked successfully for every heat load in all orientations. For each heat power input, all the temperatures increased until they reached a steady-state condition, as expected. Usually, the startup is observed when the vapor reaches the condenser, with increasing temperatures, as noticed for both devices. Startup problems can be expected for low power input levels, which is not the case of the present research, as the tests were performed always under high power inputs.

The comparison between Figures 6a and 6c, for the round, and Figures 6b and 6d, for grooved PHPs, shows that their performances were similar for operation in gravity-assisted or horizontal positions (the curves present equivalent behaviors). However, large temperature oscillations were observed for devices working at against-gravity orientation (Figure 6e and 6f) for power inputs up to 1200 W. After that, the temperatures assume the same trend as the other two positions. In other words, as the heat load increases, the lower is the gravity influence.

Remarkable improvements in the heat transfer characteristics were observed comparing the grooved PHP with the round one: a rise in the temperature of the adiabatic section, higher temperature homogeneity of each PHP region and lower temperature oscillations.

The increased adiabatic region temperature showed that the heat delivered in the evaporator reached this section more easily. Besides, the decrease of the temperature difference among all regions showed that this heat also gets to the condenser section more efficiently for the grooved PHP.

The temperature variations among the same region for all power input levels are lower for the grooved than for the round PHP. Figure 6 shows that all the red curves (evaporator temperatures) are very close to each other in the grooved PHP. This same observation can be made to all the green curves (adiabatic section) and the blue curves (condenser). For the round PHP, increasing the power input level, the scattering of the temperature curves within each section gets larger.

Another expressive difference is observed in the temperature oscillations that tend to be lower for the grooved PHP, especially in the horizontal and gravity-assisted positions. This difference can be related to the capillary action of the sharpened grooves in the PHP, which spread the working fluid in the evaporator more efficiently. Besides, these grooves also acted as nucleation sites for vapor bubbles, causing a uniform liquid-vapor phase change in the entire evaporator.

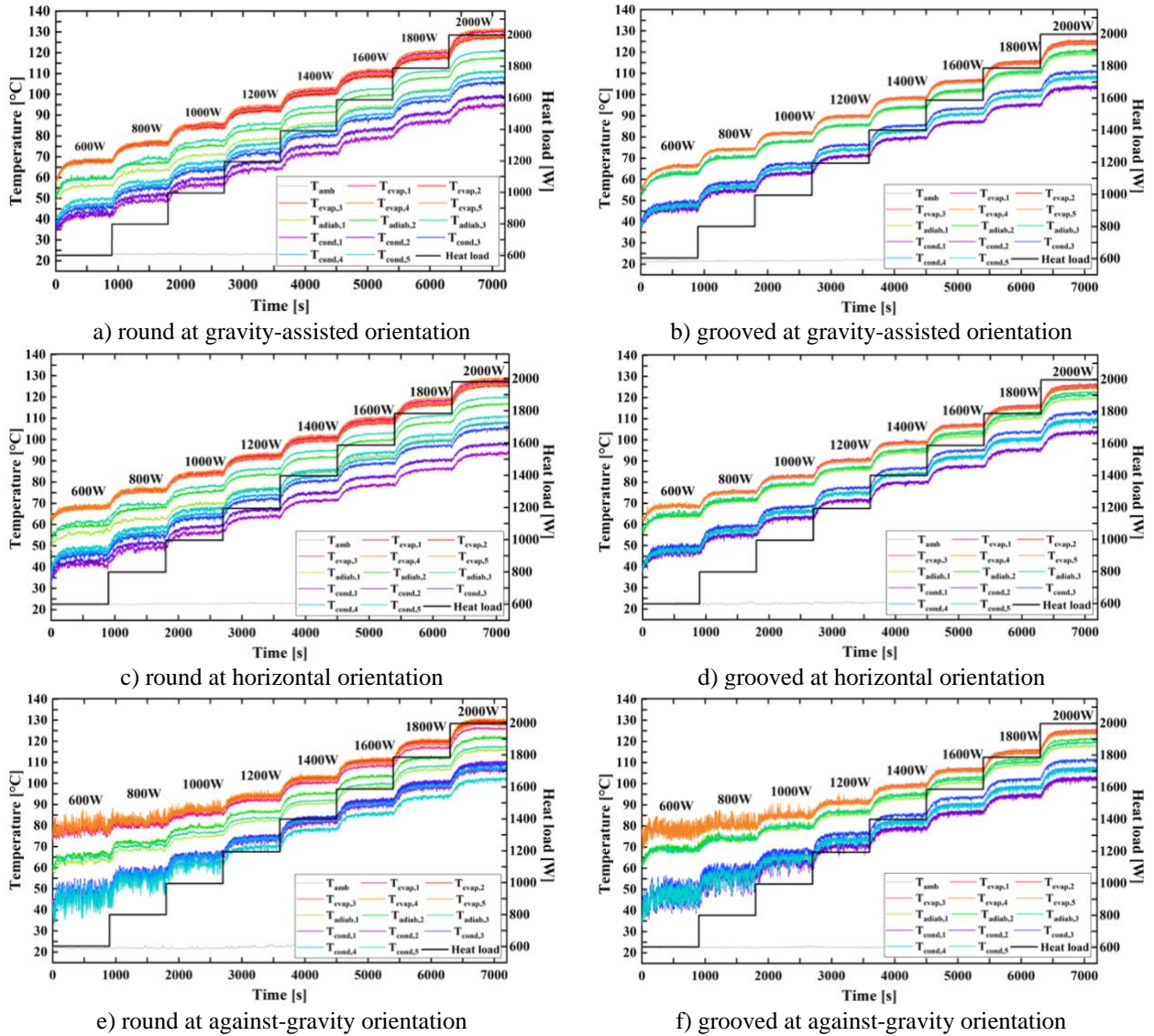


Figure 6. Temperature distribution during steady operation.

### 3.2 Average temperatures in steady-state

To analyze more carefully the thermal performance of the studied devices, the steady-state average temperatures of each region of the PHPs were calculated and are presented in Figure 7 as a function of the heat load (and heat flux). At the evaporator of the round PHP, the mean temperature varied from 68 °C at 600 W to 129.1 °C at 2000 W. At the adiabatic zone, it varied from 58.6 to 116.5 °C and, at the condenser, this variation was from 45.5 to 103.6 °C. For the grooved PHP, the mean temperature variation at the evaporator was from 66.4 to 124.4 °C, at the adiabatic zone from 62.9 °C to 119.8 °C and the condenser from 47.2 °C and 106.8 °C, all these temperatures for power inputs of 600 W and 2000 W, respectively. For the application in actual electronic systems, it can be considered that the evaporator's temperature is the most important one, as this section is supposed to be coupled to the electronic component, which temperature is to be controlled. The evaporator of the round PHP always presented higher temperature levels when compared to the grooved one, for all power inputs and testing inclinations. The difference was around 5 °C, from 1000 W to 2000 W in the vertical position. In horizontal, this difference could decrease to 1.5 °C, for some power input levels. In the inverted position, for most of the heat loads, the round PHP presented higher evaporator temperatures, with differences of 3 or 4 °C. Although, at first sight, this difference may seem small, in actual electronic applications, these temperature reductions can represent a significant improvement in the component's life cycle (Lakshminarayanan and Sriraam, 2014).

Figure 7 shows that the temperatures of the adiabatic and the condenser sections of the grooved PHP were closer to the evaporator temperatures, at gravity-assisted and horizontal positions (mentioned before). In the against-gravity orientation, both PHPs presented almost the same temperatures in the condenser and adiabatic sections. In general, the mean temperatures of Figure 7 shows that the grooved PHP exhibited better thermal performance.

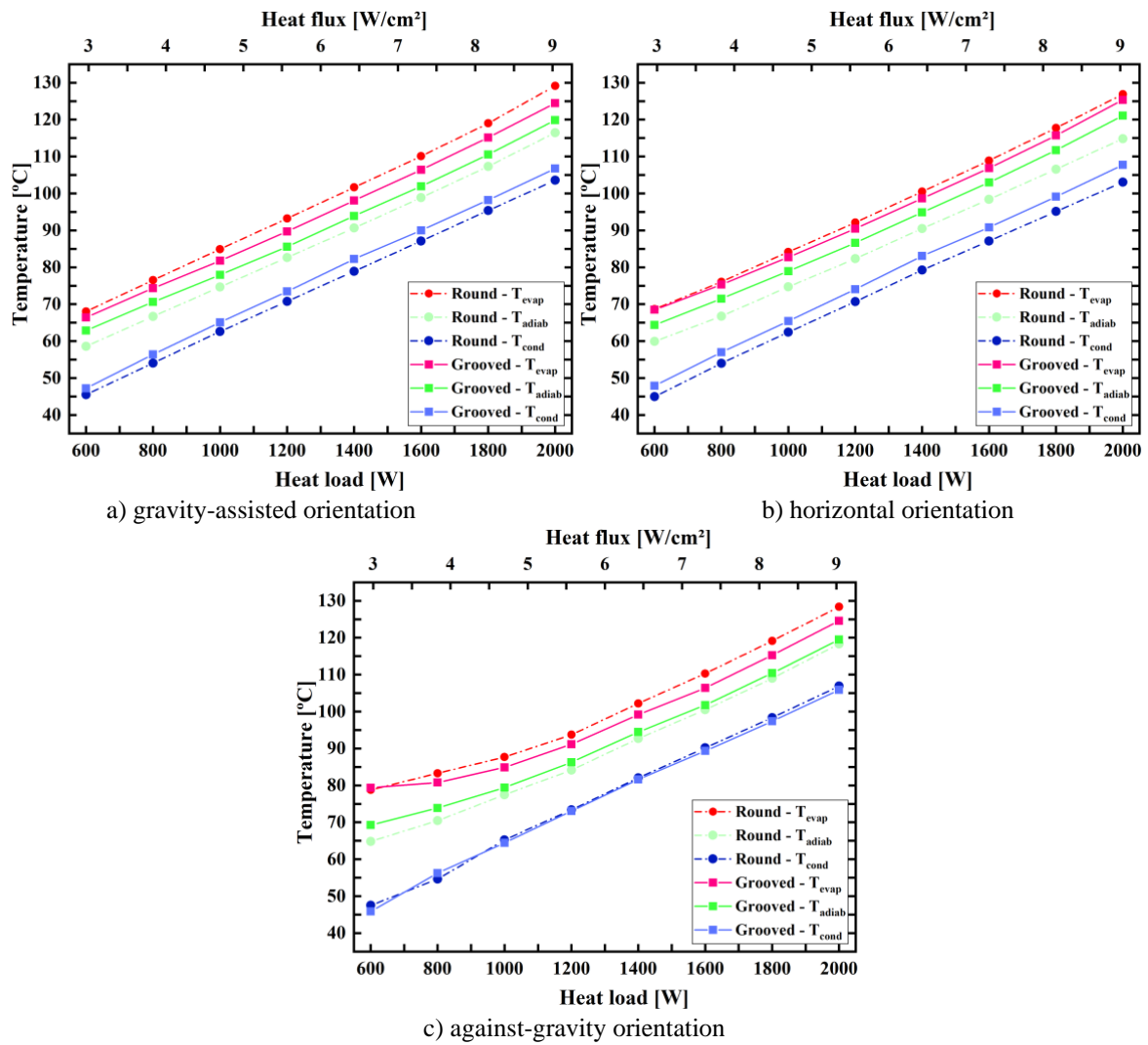


Figure 7. The average temperature of the evaporator ( $T_{evap}$ ), adiabatic section ( $T_{adiab}$ ), and condenser ( $T_{cond}$ ).

### 3.3 Temperature amplitude

As noticed before, the lateral grooves improved the temperature homogeneity inside the three regions of the grooved PHP, with smaller temperature ranges when compared to the round PHP. Figure 8 shows the amplitudes of the temperature variations (maximum minus minimum) in the evaporator and condenser regions of both PHPs. It is observed that the evaporator temperature amplitudes of grooved PHP were much smaller than those of round one, increasing slowly with heat load, reaching around 1  $^{\circ}C$ , being almost insensitive to the testing orientation. For the round channel PHP, the temperature amplitude increase is much more sensitive to the heat load and the orientation: the evaporator amplitudes vary from 2.5 to 4.5  $^{\circ}C$ , from 1.5 to 3.5  $^{\circ}C$ , and from 1 to 3  $^{\circ}C$  for the against-gravity, gravity-assisted and horizontal positions, respectively.

The condenser temperature amplitude shown in Figure 8 is also different for both PHP configurations. Although they increase with the power input, the maximum temperature amplitude for the round PHP was about 17  $^{\circ}C$ , for gravity-assisted and horizontal and 8  $^{\circ}C$  for against-gravity orientations. Meanwhile, the condenser temperature amplitude of the PHP with grooves achieves just the maximum of 8  $^{\circ}C$ .

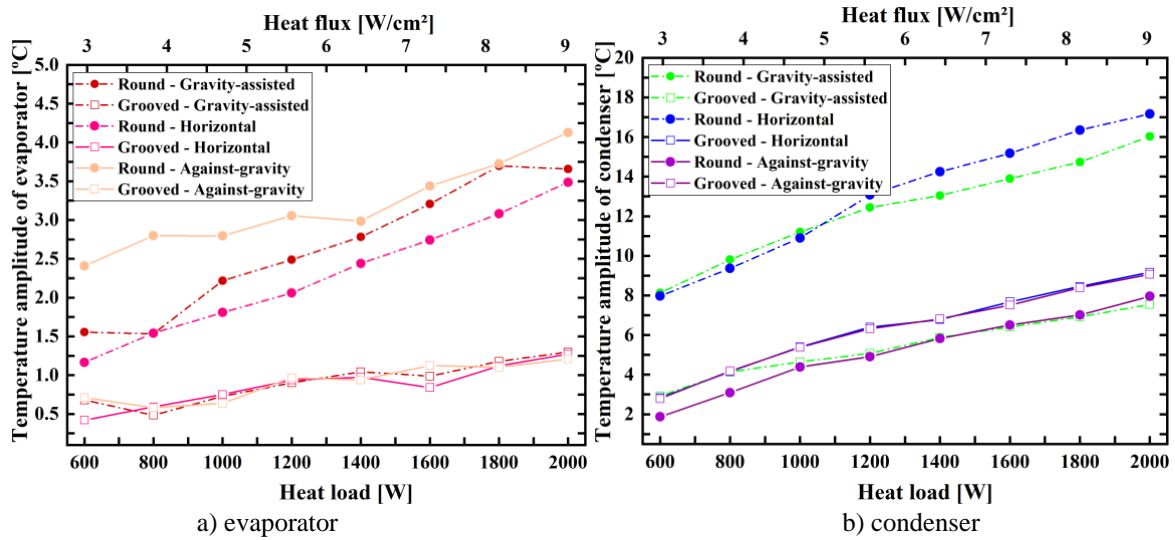


Figure 8. Temperature amplitude (difference between the maximum and minimum) for the evaporator and condenser.

### 3.4 Thermal resistance

Maybe, the overall thermal resistance is the most standard method used to analyze the thermal performance of a PHP.

Figure 9 presents the thermal resistance of the PHP as a function of the heat load for the device operating in gravity-assisted, horizontal, and against-gravity orientations. Tests of the empty PHPs showed a thermal resistance of  $R_t = 0.51 \pm 0.02$  °C/W, which corresponds to only the conduction as heat transfer phenomenon. It should be noted that both devices worked successfully as a pulsating heat pipe, from the first power input level tested, which was already high, of 600 W. As the heat input increases, both devices show better thermal performance.

Figure 9 shows that the grooved PHP had a lower thermal resistance and, therefore, a higher overall heat transfer capacity in all orientations. However, for high power input levels (2000 W), both the round and grooved PHP presented low thermal resistance of 0.013 °C/W and 0.009 °C/W, respectively, in the gravity-assisted orientation. Actually, the devices worked similarly in all positions for heat loads higher than 1200 W, even when operating against gravity. For this reason, these PHP appears to be a good alternative for microgravity applications.

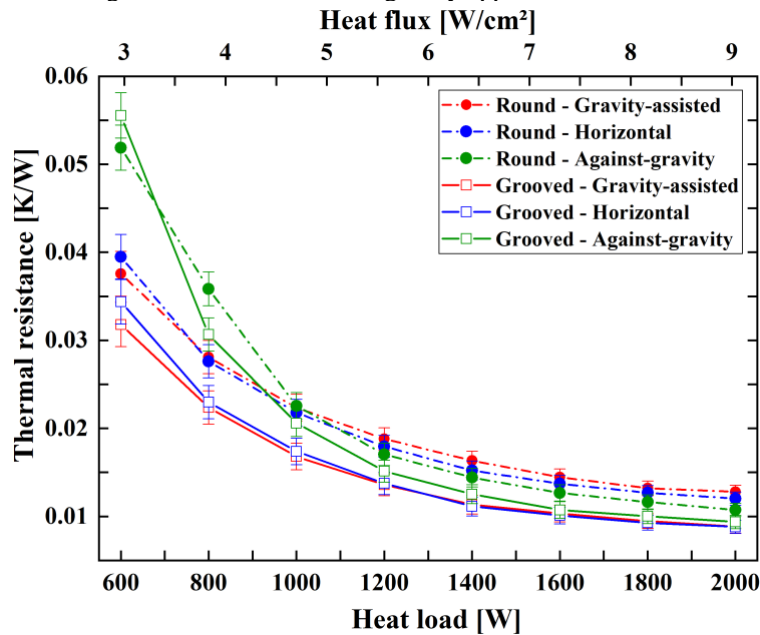


Figure 9. Comparison of the thermal resistances.

It is interesting to highlight that literature studies concerning new groove geometries for PHP show that grooves work better for low heat loads when compared to more ordinary shapes (Kim and Kim, 2018). However, the present study shows that the thermal enhancement of grooved PHP might be found in high heat input levels, as larger as 2000 W, which means that the PHP may be applied in many possible conditions.

#### 4. CONCLUSIONS

In this research, a new channel geometry was experimentally analyzed for flat plate pulsating heat pipes in high heat load operating conditions. This novel geometry consists of a round cross-section with ultra-sharp lateral grooves, locating in the evaporator. If the diffusion bonding process is used, this geometry can be easily fabricated. The thermal performance was compared to ordinary flat PHP with a round cross-section channel. The dissipated power varied from 600 to 2000 W, a value higher than the PHP's working conditions described in the literature, for three positions (gravity-assisted, horizontal, and against-gravity orientation).

For large heat loads, both PHPs work successfully, able to transfer up to 2000 W. As the dissipated power increases, the steady-state temperatures also grow and the overall thermal resistance reduces. The thermal tests performed showed that the tested devices are suitable for high power dissipation applications, with the gravity influence negligible for powers beyond 1200 W, for any orientation. For power input lower than 1200 W, gravity influence was observed only for the against-gravity position.

The grooved pulsating heat pipe presents the following advantages when compared to the round one:

- The temperature of the adiabatic section is higher, closer to the evaporator temperature.
- The grooved PHP presents higher temperature homogeneity for the three sections. In the horizontal testing configuration, the temperature amplitudes decreased from 17 to 8 °C in the condenser and from 3.5 to 1 °C in the evaporator.
- The grooved PHP presents lower temperature oscillations, especially in horizontal and gravity-assisted operating conditions.
- As a result of the better heat transfer characteristics, the grooved PHP has lower evaporator average temperatures for all operating inclinations, with a difference of around 5 °C in the gravity-assisted position, which can be crucial for life cycle of electronic components.
- This better thermal performance results in lower thermal resistances observed for the device operating in all orientations and heat loads. The maximum thermal resistance decreased by 60% in the gravity-assisted and horizontal positions and 20% in the against-gravity orientation.

As a conclusion, it can be stated that both PHPs, constructed from diffusion bonding technique, can be considered satisfactory alternatives for large heat transfer applications. As they operated well in all tested orientations, even against gravity, they are great options for microgravity conditions. This is an important contribution of the present work to the state of the art, since PHP studies for high power dissipations are still very few. Moreover, the thermal improvement reached by this simple, low-cost channel modification is expressive, as it significantly reduces the device operating temperature, increasing the thermal stability of the electronic devices. These effects are consequences of the capillary effect of the ultra-sharp grooves, which keeps all the evaporator wet and helps in the creation of bubble nucleate sites, improving evaporation of the working fluid.

#### 5. ACKNOWLEDGEMENTS

The authors acknowledge CNPq (Conselho Nacional de Desenvolvimento Científico e Tecnológico) for providing scholarships for the graduation students and UFSC (Universidade Federal de Santa Catarina) for their support to the present research.

#### 6. REFERENCES

- Betancur-Arboleda, L., Hulse, P., Melian, I., Mantelli, M.H., 2020. "Diffusion bonded pulsating heat pipes: fabrication study and new channel proposal". *Journal of Brazilian Society of Mechanical Engineers*, Vol. 42, pp. 466.
- Cai, Q., Chen, C.L., Asfia, J.F., 2006. "Heat transfer enhancement of planar pulsating heat pipe device". In *Proceedings of 2006 ASME International Mechanical Engineering Congress and Exposition, IMECE2006 - Heat Transfer*. American Society of Mechanical Engineers (ASME), Chicago, IL, United States.
- Czajkowski, C., Nowak, A.I., Błasiak, P., Ochman, A., Pietrowicz, S., 2020. "Experimental study on a large scale pulsating heat pipe operating at high heat loads, different adiabatic lengths and various filling ratios of acetone, ethanol, and water". *Applied Thermal Engineering*, Vol. 165, pp. 114534.
- Facin, A., Betancur, L., Mantelli, M., Florez, J.P., Coutinho, B.H., 2018. "Influence of channel geometry on diffusion bonded flat plate pulsating heat pipes". In *19th International Heat Pipe Conference and 13th International Heat Pipe Symposium*. Pisa, Italy, June 10-14.
- Holman, J.P., 2011. *Experimental methods for engineers*, 8th ed, McGraw-Hill. New York, USA.
- Hosoda, M., Nishio, S., Shirakashi, R., 1999. "Meandering closed loop heat transport tube (propagation phenomena of vapor plug)". In *5th ASME/JSME Joint Thermal Engineering Conference*. San Diego, USA.
- Karimi, G., Culham, J.R., 2004. "Review and assessment of pulsating heat pipe mechanism for high heat flux electronic cooling". In *2004 Inter Society Conference on Thermal Phenomena*, pp. 52–59.
- Khandekar, S., Schneider, M., Schäfer, P., Kulenovic, R., 2003. "Thermofluid dynamic study of flat plate closed loop

- pulsating heat pipes". *Microscale Thermophysical Engineering*, Vol. 6, pp. 303–317.
- Kim, W., Kim, S.J., 2018. "Effect of reentrant cavities on the thermal performance of a pulsating heat pipe". *Applied Thermal Engineering*, Vol. 133, pp. 61–69.
- Lakshminarayanan, V., Sriraam, N., 2014. "The effect of temperature on the reliability of electronic components". In *IEEE International Conference on Electronics, Computing and Communication Technologies (CONECCT)*. Bangalore, pp. 1-6.
- Laun, F.F., Lu, H., Ma, H.B., 2015. "An experimental investigation of an oscillating heat pipe heat spreader". *Journal of Thermal Science Engineering Applications*, Vol. 7, pp. 021005.
- Ma, H., 2015. *Oscillating Heat Pipes*. Springer New York. New York, NY.
- Qu, J., Li, X., Xu, Q., Wang, Q., 2017. "Thermal performance comparison of oscillating heat pipes with and without helical micro-grooves". *Heat Mass Transfer*, Vol. 53, pp. 3383-3390.
- Yoon, A., Kim, S.J., 2014. "The effect of substrate conduction on the thermal performance of a flat plate pulsating heat pipe". In *10th International Conference on Heat Transfer, Fluid Mechanics and Thermodynamics*. Orlando, Florida, pp. 1411–1416.

## 7. RESPONSIBILITY NOTICE

The authors are the only responsible for the printed material included in this paper.